Biomedicine & Pharmacotherapy 163 (2023) 114760

Contents lists available at ScienceDirect

Biomedicine & Pharmacotherapy

journal homepage: www.elsevier.com/locate/biopha

Tigecycline reduces tumorigenesis in colorectal cancer via inhibition of cell proliferation and modulation of immune response

Antonio Jesús Ruiz-Malagón [a,b,1], Laura Hidalgo-García [a,b,1], María Jesús Rodríguez-Sojo [a,b], José Alberto Molina-Tijeras [a,b], Federico García [b,c,d], Patricia Diez-Echave [a,b], Teresa Vezza [a,b], Patricia Becerra [b,e], Juan Antonio Marchal [b,f,g], Eduardo Redondo-Cerezo [b,h], Martin Hausmann [i], Gerhard Rogler [i,j], José Garrido-Mesa [k,2,*], María Elena Rodríguez-Cabezas [a,b,3,**], Alba Rodríguez-Nogales [a,b,4], Julio Gálvez [a,b,l,4]

[a] Department of Pharmacology, Center for Biomedical Research (CIBM), University of Granada, 18071 Granada, Spain
[b] Instituto de Investigación Biosanitaria de Granada (ibs.GRANADA), 18012 Granada, Spain
[c] Servicio Microbiología, Hospital Universitario Clínico San Cecilio, 18100 Granada, Spain
[d] Ciber de Enfermedades Infecciosas, CiberInfecc, Instituto de Salud Carlos III, 28029 Madrid, Spain
[e] Servicio de Anatomía Patológica, Hospital Universitario Clínico San Cecilio, 18014 Granada, Spain
[f] Biopathology and Regenerative Medicine Institute (IBIMER), Centre for Biomedical Research (CIBM), University of Granada, E-18100 Granada, Spain
[g] Department of Human Anatomy and Embryology, Faculty of Medicine, University of Granada, Granada E-18016, Spain
[h] Servicio de Aparato Digestivo. Hospital Universitario Virgen de las Nieves, Granada, Spain
[i] Department of Gastroenterology and Hepatology, University Hospital Zurich, University of Zurich, Rämistrasse 100, 8091, Zurich, Switzerland
[j] Zurich Center for Integrative Human Physiology (ZIHP), University of Zurich, 8057, Zurich, Switzerland
[k] The William Harvey Research Institute, Barts and the London School of Medicine, Queen Mary University of London, London, UK
[l] Centro de Investigación Biomédica en Red de Enfermedades Hepáticas y Digestivas (CIBEREHD), Instituto de Salud Carlos III, 28029 Madrid, Spain

ARTICLE INFO

Keywords:
Colitis-associated colorectal cancer
Tigecycline
β-catenin
Cytotoxic T lymphocytes
Microbiota

ABSTRACT

Background: and Purpose: Colorectal cancer (CRC) is one of the cancers with the highest incidence in which APC gene mutations occur in almost 80% of patients. This mutation leads to β-catenin aberrant accumulation and an uncontrolled proliferation. Apoptosis evasion, changes in the immune response and microbiota composition are also events that arise in CRC. Tetracyclines are drugs with proven antibiotic and immunomodulatory properties that have shown cytotoxic activity against different tumor cell lines.
Experimental approach: The effect of tigecycline was evaluated in vitro in HCT116 cells and in vivo in a colitis-associated colorectal cancer (CAC) murine model. 5-fluorouracil was assayed as positive control in both studies.
Key results: Tigecycline showed an antiproliferative activity targeting the Wnt/β-catenin pathway and down-regulating STAT3. Moreover, tigecycline induced apoptosis through extrinsic, intrinsic and endoplasmic reticulum pathways converging on an increase of CASP7 levels. Furthermore, tigecycline modulated the immune response in CAC, reducing the cancer-associated inflammation through downregulation of cytokines expression. Additionally, tigecycline favored the cytotoxic activity of cytotoxic T lymphocytes (CTLs), one of the main

Abbreviations: ATF6, activating transcription factor 6; AOM, azoxymethane; BAX, Bcl-2-associated X protein; DDIT3, C/EBP homologous protein; CSCs, cancer stem cells; CAC, colorectal associated-cancer; CRC, Colorectal cancer; DSS, dextran sulfate sodium; DAI, disease activity index; ER, endoplasmic reticulum; HSPA5, immunoglobulin heavy chain-binding protein; IBD, inflammatory bowel disease; JNK, Jun-N-terminal kinase; MOMP, membrane permeabilization; MLN, mesenteric lymph nodes; MMP, metalloproteinases; PCoA, Principal Coordinates Analysis; RDP, Ribosomal Database Project; tBID, Truncation of BID; TP53, tumor protein 53; CTNNB1, β-catenin.

* Correspondence to: Department of Medical & Molecular Genetics, School of Basic and Medical Biosciences, Faculty of Life Sciences & Medicine, King's College London, UK.
** Corresponding author at: Department of Pharmacology, Center for Biomedical Research (CIBM), University of Granada, 18071 Granada, Spain.
E-mail addresses: j.garrido@kcl.ac.uk (J. Garrido-Mesa), merodri@ugr.es (M.E. Rodríguez-Cabezas).
[1] Both authors contributed equally to the study.
[2] ORCID: https://orcid.org/0000–0001-6420–9055
[3] ORCID: https://orcid.org/0000–0001-9085–8147
[4] Both authors contributed equally to the supervision of the study.

https://doi.org/10.1016/j.biopha.2023.114760
Received 7 March 2023; Received in revised form 13 April 2023; Accepted 20 April 2023
Available online 27 April 2023

immune defenses against tumor cells. Lastly, the antibiotic reestablished the gut dysbiosis in CAC mice increasing the abundance of bacterial genera and species, such as *Akkermansia* and *Parabacteroides distasonis*, that act as protectors against tumor development. These findings resulted in a reduction of the number of tumors and an amelioration of the tumorigenesis process in CAC.
Conclusion and implications: Tigecycline exerts a beneficial effect against CRC supporting the use of this antibiotic for the treatment of this disease.

1. Introduction

Colorectal cancer (CRC) is the second most diagnosed cancer in women and the third in men. Moreover, CRC is the third most deadly them, responsible for nearly a million deaths in 2020 (GLOBOCAN, 2020). Whilst recent developments/advances in its screening and treatment have reduced the mortality, the survival rate remains low, especially for metastatic CRC, with a 5-year survival rate of 12% [1]. Furthermore, an elevated percentage of patients do not respond to the current treatments or show important adverse effects, so the development of new adjuvant therapies against CRC is still necessary. Different risk factors contribute to the development of CRC, from the patient's genetic background to aging, intestinal inflammation, diet and other environmental factors [2]. The accumulation of genetic mutations leads to an altered balance between the activation of oncogenes and the reduction of tumor suppressor genes [3]. For instance, the mutations in the APC gene in the intestinal epithelium are an early event that occurs in almost 80% of CRC patients [4] leading to β-catenin aberrant activation and increasing cell proliferation [5]. In addition, a proinflammatory environment contributes to potentiate cell proliferation, angiogenesis and cancer progression [6]. In fact, patients with inflammatory bowel disease (IBD) have a significantly elevated risk of CRC development [7].

Moreover, CRC tumorigenesis and progression have been clearly associated with an imbalanced gut microbiome, commonly termed as dysbiosis. Thus, changes in gut microbiome abundance have been described in patients with CRC [8] evidencing a critical role for specific bacteria in colon tumorigenesis, like *Fusobacterium nucleatum* and *Bacteroides fragilis* [9], as well as, a depletion of some bacterial species like *Faecalibacterium prausnitzii* [10].

Considering the involvement of the microbiome in the initiation and progression of CRC, the modulation of the gut microbiota can be considered as a potential strategy for prevention and treatment of CRC [11]. In this regard, tetracyclines are a family of broad-spectrum antibiotics that have shown beneficial effects against intestinal inflammation [12] since they present immunomodulatory properties in addition to their antibiotic activity, being tigecycline an example. Besides, these antibiotics have shown cytostatic and cytotoxic activity against different tumor cell lines [13], as well as against metastasis due to their ability to inhibit metalloproteinases (MMP) [14]. The effect of the tetracyclines in cancer has been extensively studied and many reports have revealed additional antitumoral properties including antiproliferative properties [15,16], proapoptotic [17,18], antimetastatic activity [19,20] and antiangiogenic effects [21–27]. Among tetracyclines with antitumor activities, tigecycline is one the most promising candidates for cancer treatment. Tigecycline, the first member of the glycylcycline bacteriostatic agents, was developed for the treatment of polymicrobial multidrug-resistant infections and it has been approved to treat complicated infections in the clinic because of its expanded-spectrum antibiotic potential, existing recent evidence suggesting that tigecycline may also be effective in the treatment of severe *Clostridioides difficile* infection [28]. Its antibacterial mode of action is the inhibition of bacterial protein translation via reversible binding to a helical region (H34) on the 30 S subunit of bacterial ribosomes. Besides, an increasing number of reports have pointed out the anti-tumor effects of tigecycline. These effects on cancer are mediated by the modulation of different signaling pathways and mitochondrial functions in cancer cells. Thus, tigecycline has shown an antitumor effect on pancreatic ductal adenocarcinoma and multiple myeloma through the inhibition of cell proliferation, migration, and invasion [25,29].

Therefore, it is interesting to explore the potential application of tigecycline for the treatment of CRC. In the present study, we evaluated the antitumor effect of tigecycline using a combination of in vitro and in vivo studies carried out on tumoral cells and azoxymethane (AOM) / dextran sulfate sodium (DSS) murine model, respectively.

2. Material and methods

2.1. Chemicals, cell culture and treatment

The human colon cancer cell lines HCT116 and Caco-2 were obtained from the Cell Culture Unit of the University of Granada (Granada, Spain). NCM356 human colonic epithelial cells were kindly provided by Laura Medrano González and Ezra Aksoy (William Harvey Research Institute, Queen Mary University of London, London, UK).

Cells were cultured and treated with tigecycline (Tygacil®, Pfizer, New York, USA), Wnt3a (Sigma-Aldrich, Madrid, Spain) and 5-fluorouracil (5-FU) (Accord Farma, Polanco, Mexico) as described in Supplementary Material and Methods. RNA and cytoplasmic and nuclear proteins were isolated for Taqman qPCR and Western blot, respectively.

2.2. Cell proliferation assay

HCT116 and NCM356 cells were treated with different doses of tigecycline (1–75 μM) or 5-FU (5–100 μM) for 48 h. After that, cell viability was measured using an MTS assay (CellTiter 96® AQueous One Solution Cell Proliferation Assay, Promega, Madison, USA) according to the manufacturer's instructions.

2.3. Colony formation assay

HCT116, Caco-2 and NCM356 cells were plated into 6-well plates at 200 cells/well for HCT116 and 400 cells/well for Caco-2 and NCM356. From the following day, fresh media was added supplemented with different doses of tigecycline and 5-FU, every 48 h for 1 week, when the media was removed, the cells were fixed with absolute ethanol and the colonies were stained with 2.3% crystal violet and counted with ImageJ software (Free Software Foundation Inc) after taking the images.

2.4. Annexin V and propidium iodide (PI) assay

Apoptosis and necrosis were evaluated by flow cytometry using FITC Annexin V apoptosis detection kit with PI (Immunostep, Salamanca, Spain). HCT116 cells were treated with different concentrations of tigecycline (1–50 μM) for 48 h. After the treatment, attached cells and those present in the supernatant were collected, washed with cold PBS and stained with FITC-Annexin V and PI. Labeled cells were acquired on a BD FACsAria Ill (BD Biosciences, Becton, Dickinson and Company, Franklin Lakes, NY, USA) and data were analyzed using the FlowJo v10.6.2 software (FlowJo LLC, Ashland, OR, USA).

2.5. TUNEL assay

In order to confirm the apoptotic capacity of the treatments, a TUNEL

assay was carried out in HCT116 cells treated with tigecycline or 5-FU for 48 h (n = 3) with the TUNEL assay kit-HRP DAB ab206386 (Abcam, Cambridge, UK) following the manufacturer's instruction.

Apoptosis was also evaluated using the DeadEnd Fluorometric TUNEL system (Promega, Madison, USA) in colonic tissue sections following the manufacturer's indications.

Full description of the methods can be found in Supplementary Material and Methods.

2.6. CAC murine model, DAI evaluation and macroscopic data analysis

All mice studies were performed following the 'Guide for the Care and Use of Laboratory Animals' as promulgated by the National Institute of Health and the protocols approved by the Ethic Committee of Laboratory Animals of the University of Granada (Spain) (Ref. No.23/10/2019/174). The facility of the animal unit was managed by professional personnel, following the Animals in Research: Reporting In Vivo Experiments guidelines (ARRIVE guidelines). C57Bl/6 J female mice (7–9 weeks old) from Charles River (Barcelona, Spain) were housed in groups of five mice in each makrolon cage, with an air-conditioned atmosphere, a 12 h light-dark cycle and provided with free access to tap water and food. They were subjected to a process of CAC induction by administering one intraperitoneal initial dose of AOM (Sigma-Aldrich, Madrid, Spain) at 10 mg/kg followed by three cycles of DSS (36–50 kDa, MP Biomedicals, Illkirch Cedex, France) added in the drinking water. Each DSS cycle consisted of 2% DSS for 1 week followed by a recovery period of 2 weeks with normal drinking water. Mice were divided into five groups: healthy control, colorectal associated-cancer (CAC) control, and three CAC groups treated daily with tigecycline 25 mg/kg or tigecycline 50 mg/kg by oral gavage or every three days with 5-FU 15 mg/kg intraperitoneally. The treatment started 50 days after the beginning of the assay, on the day of initiation of the third cycle of DSS and lasted for 7 weeks. The control groups received PBS following the same protocol.

A detailed description of the procedures can be found in Supplementary Material and Methods. Briefly, the disease activity index (DAI) [30] was determined daily in each DSS cycle, and the day before euthanasia, both tumor number and size was assessed via colonoscopy and a tumor score was given as described by Becker C et al., [31] by a blind observer.

After 14 weeks of the beginning of the assay, mice were sacrificed and spleen, mesenteric lymph nodes (MLN) and colon were aseptically collected. The bowels were open longitudinally, the macroscopic tumors were counted, and images were acquired for measuring the size of each tumor with the ImageJ software. At the endpoint, colon samples were taken for RT-qPCR, Western blot, flow cytometry and fixed for histological studies. A detailed description of the procedures can be found in Supplementary Material and Methods.

2.7. Microbiota

Faeces samples from each mouse were aseptically collected on the end-point day of the assay. Stool DNA was isolated using the QIAamp PowerFecal Pro DNA Kit (Qiagen, Hilden, Germany). Total DNA was amplified and a library for the V4–V5 region of 16 S rRNA was constructed in accordance with the 16 S Metagenomic Sequencing Library Preparation Illumina protocol. Sequencing was executed using the MiSeq 2 × 300 platform (Illumina Inc., San Diego, CA, USA) in accordance with the manufacturer's instructions.

The resulting sequences were completed, quality-filtered, clustered, and taxonomically assigned on the basis of 97% similarity level against the RDP (Ribosomal Database Project) [32] by using the QIIME2 software package (2021.11 version) and "R" statistical software package (version 3.6.0; https://www.r-project.org/). Alpha diversity and beta diversity were determined by the q2-diversity plugin in QIIME2. Differential abundance analysis was performed using the Wald test implemented DESeq2 v1.30.1 as previously described [33] within the "R" statistical software (version 4.0; https://www.r-project.org/). Healthy and the three treated groups were compared with the control CAC-group and *EnhancedVolcano* package was used for constructing volcano-plots. Log2-fold-change (Log2FC) normalized values and the adjusted P-value (*Padj)* were used to construct Venn diagrams (Limma package) of differentially microbial communities up-regulated (log2FC>1.5 and *Padj < 0.05)* and downregulated (log2FC<1.5 and *Padj < 0.05)* among groups.

2.8. Statistical and correlation analysis

Statistical analysis was performed using the GraphPad Prism version 7 software (GraphPad Software, Inc, San Diego, CA, USA) with statistical significance set at $P < 0.05$. All data are represented as mean (SEM) of at least 3 independent experiments/biological replicates unless otherwise stated in the figure legends. The Mann-Whitney U test for nonparametric data was used for the analysis of the DAI. For the rest of the data, multiple comparisons between groups were performed using the one-way ANOVA followed by Tukey's test.

A heat map depicting the macroscopic parameters, molecular changes, and patterns of microbial abundance of untreated CAC mice and those treated with both doses of tigecycline was constructed within the "R" statistical software using the "Hmisc" and "ggplot2" packages. Spearman's correlations of each parameter were previously calculated with "R" software.

3. Results

3.1. Tigecycline exerts an antiproliferative effect in vitro

The antiproliferative effect of tigecycline was evaluated by performing clonogenic and MTS assays in the colon cancer cell lines HCT116 and Caco-2, as well as in the epithelial cell line derived from the normal colon mucosa NCM356. Treatment with tigecycline reduced proliferation (Fig. 1 A) and clonogenic capacity (Fig. 1B) of all the cell lines tested in a dose-dependent manner, similarly to 5-FU. However, 5-FU showed more cytotoxic effect as observed in the MTS assay (Fig. 1A). These results were confirmed in HCT116 cells by immunofluorescence assay using the antibody anti-MKI67 (Fig. 1C).

Then, we studied the molecular mechanisms involved in the antiproliferative effects of tigecycline, focusing on the role of β-catenin (CTNNB1), a mediator in the Wnt signaling pathway, involved in the development of several types of cancer, including CRC [34].

Tigecycline and 5-FU reduced nuclear CTNNB1 as well as increased cytoplasmic CTNNB1, thus lowering nuclear/cytoplasmic ratio in comparison with non-treated cells (Fig. 2A). Consequently, tigecycline hinders CTNNB1 nuclear translocation, maybe increasing cytoplasmic CTNNB1 phosphorylation (Fig. 2A). Moreover, they also reduced MYC levels (Fig. 2A), downstream of the CTNNB1 pathway. In addition, tigecycline also inhibited STAT3 activation (Fig. 2A), which promotes nuclear accumulation of CTNNB1 [35].

To confirm these results the Wnt/β-catenin pathway was stimulated with Wnt3a in HCT116 cells, which caused a reduction of CTNNB1 phosphorylation and increased nuclear CTNNB1 (Fig. 2B), thus resulting in upregulated *AXIN2* and *MYC* transcription (Fig. 2C). However, tigecycline and 5-FU enhanced CTNNB1 phosphorylation and lowered its nuclear translocation, evidenced by the lower nuclear CTNNB1 levels in treated cells (Fig. 2B). Downregulated expression of CTNNB1 target genes, *MYC* and *AXIN2,* was also observed with tigecycline and 5-FU (Fig. 2C). Therefore, we confirmed that tigecycline and 5-FU act as inhibitors of the Wnt/β-catenin pathway in tumor cells, both in basal and Wnt3a-stimulated proliferation.

3.2. Tigecycline shows pro-apoptotic effects in colon cancer cell lines

To evaluate the pro-apoptotic capacity of tigecycline, we used the

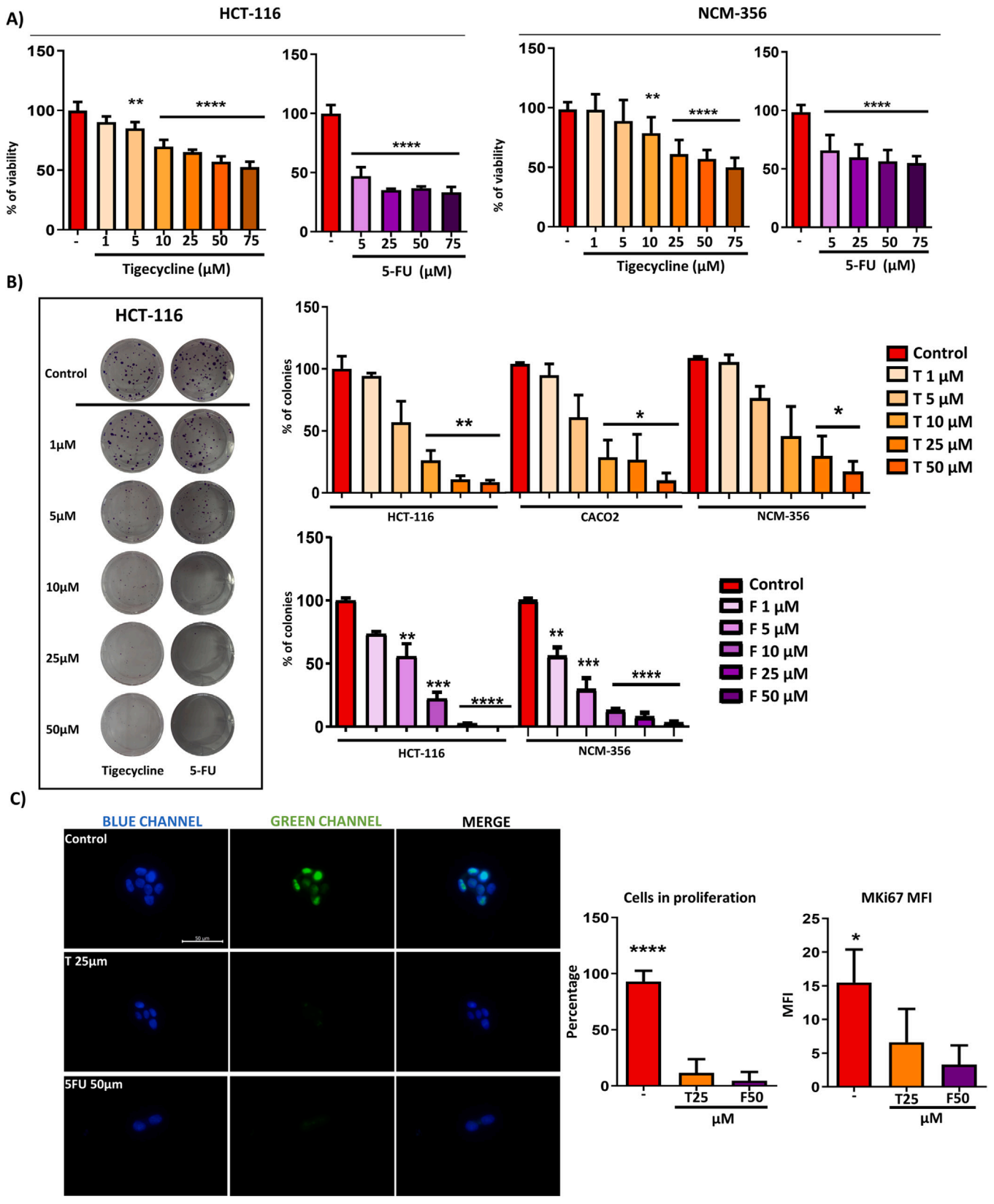

Fig. 1. In vitro anti-proliferative effect of tigecycline and 5-FU. (A) Cell proliferation evaluated by MTT assay (B) Clonogenic assay in HCT116, Caco-2 and NCM356 cell lines treated with different doses of tigecycline or 5-FU. (C) Immunofluorescence representative images of Ki67 (green) staining in HCT116 cells non-treated or treated with tigecycline or 5-FU, cells in proliferation based on ki-67 positive cells and total cells (right and up) and ki-67 mean fluorescence intensity (MFI) (right and down). Scale bar: 50 μm. Data are presented as mean ± SEM. *P < 0.05, * *P < 0.01, * **P < 0.001 vs. control.

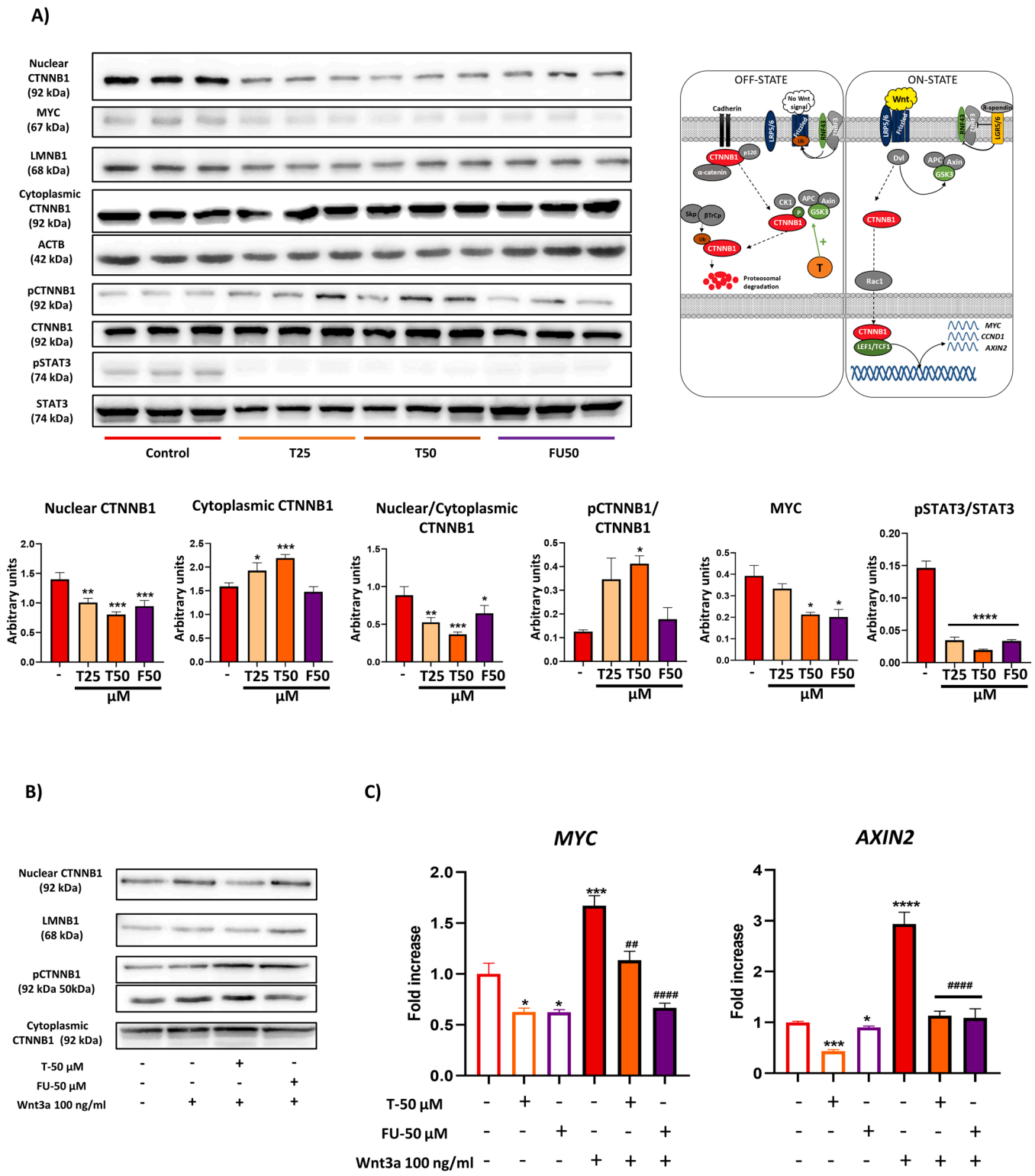

Fig. 2. Molecular mechanisms involved in the anti-proliferative effect of tigecycline and 5-FU: effect on Wnt/β-catenin pathway. (A) Impact on β-catenin nuclear and cytoplasmic levels analyzed by Western blot in basal conditions or (B) stimulated with Wnt3a (C) Effect on the expression of Wnt/β-catenin target genes in the presence or absence of Wnt. Data are presented as mean ± SEM. *P < 0.05, * *P < 0.01, * **P < 0.001, * ** *P < 0.0001 vs. control. #P < 0.05, ##P < 0.01, ###P < 0.001, ####P < 0.0001 vs. control + Wnt.

Annexin V / PI assay in HCT116 cells. We observed a dose-response effect in the percentage of $ANXV^{+}IP^{-}$ cells (Fig. 3A), thus revealing its ability to promote early apoptosis after 48 h of treatment. No significant differences in the number of late apoptotic or necrotic cells ($ANXV^{+}IP^{+}$) were found. These results were confirmed by the TUNEL assay performed in HCT116 cells, since the treatment with tigecycline significantly increased the staining of brown (apoptotic) nuclei (Fig. 3B), as did the control treatment (Fig. 3B).

Three different pathways of apoptosis have been described: the extrinsic or death receptor pathway, the intrinsic or mitochondrial

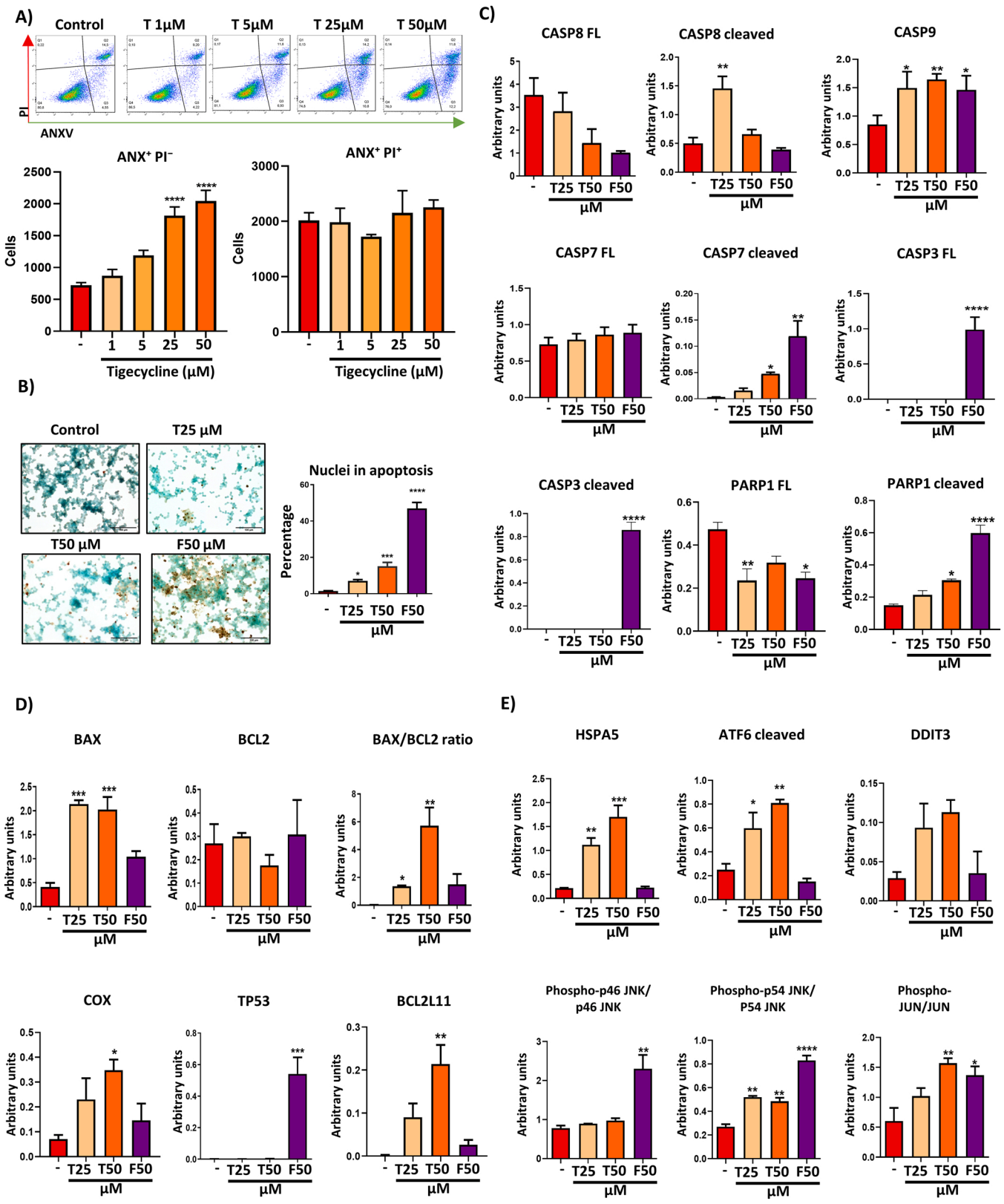

Fig. 3. Pro-apoptotic effect of tigecycline and 5-FU in vitro and molecular mechanisms involved in this effect. (A) Apoptosis study by Annexin-IP assay in HCT116 cell line. Gating strategy used to evaluate apoptosis after tigecycline treatment in vitro (up). Number of apoptotic cells after different concentrations of tigecycline (down) (B) Apoptosis evaluation of tigecycline treatment in HCT116 cells using Tunel assay. Scale bar: 100 µm (C) Impact on extrinsic apoptosis pathway (D) intrinsic apoptosis pathway (E) and endoplasmic reticulum mediated apoptosis pathway. Data are presented as mean ± SEM. *P < 0.05, **P < 0.01, ***P < 0.001, * ** *P < 0.0001 vs. control.

pathway, and a third less well-known that involves the endoplasmic reticulum (ER). We observed that the cellular pathways involved in 5-FU-mediated apoptosis were slightly different from those engaged by tigecycline (Fig. 3C-E). When considering the extrinsic pathway, tigecycline (25 μM) increased the levels of cleaved CASP8, as well as the ratio between the cleaved and the full-length form (Fig. S1A), with a trend to reduce full-length CASP8, although not significant (Fig. 3C). Subsequently, we evaluated the last steps of the extrinsic pathway. Tigecycline significantly increased CASP9 and the cleaved form of the executioner CASP7 (Fig. 3C). Levels of CASP9 and cleaved CASP7 were also increased by 5-FU, which also upregulated the levels of CASP3 and their active forms (Fig. 3C). Furthermore, the treatment of HCT116 with tigecycline significantly increased the levels of cleaved PARP1 and reduced the levels of full length PARP1 leading to a significant increment of the ratio (Figs. 3C and S1A). This action was even more intense with the 5-FU treatment (Figs. 3C and S1A). These results support that treatment with tigecycline exerts a pro-apoptotic effect, as shown by 5-FU.

Besides, tigecycline increased the levels of both BID and tBID, even though this increase was not statistically significant (Fig. S1A). Truncation of BID (tBID) by cleaved CASP8 on the mitochondrial membrane is required for the formation of pores and the release of cytochrome C oxidase (COX) to the cytosol, and it has been reported that BID acts as a link between the extrinsic pathway and the intrinsic pathway of apoptosis [36]. Interestingly, the incubation of the cells with either tigecycline or 5-FU significantly increased the levels of Bcl-2-associated X protein (BAX) and its oligomer (Fig. 3D and S1A). BAX is a member of the Bcl-2 family proteins that oligomerizes and promotes a mitochondrial outer membrane permeabilization (MOMP) [37]. BCL2 inactivates BAX and its pore-forming function, so the ratio BAX/BCL2 an indicator of the cell apoptosis state. Tigecycline or 5-FU+ did not significantly modify BCL2 levels but increased BAX/BCl2 ratio (Fig. 3D), which would promote the pore formation in the mitochondrial membrane and the release of COX. In fact, COX levels were increased in those cells incubated with tigecycline (Fig. 3D). In addition, tumor protein 53 (TP53), involved in COX release through BAX stimulation and BCL2 inhibition and, thus, favoring the formation of the apoptosome was up-regulated by 5-FU, but not by tigecycline (Fig. 3D). However, tigecycline acted downstream increasing BCL2L11 levels (Fig. S1B).

The pro-apoptotic effects of both tigecycline and 5-FU also involve the ER pathway, although in different ways (Fig. 3D and S1C). Tigecycline increased the levels of the ER-stress marker immunoglobulin heavy chain-binding protein (HSPA5) (Fig. 3E). Similarly, tigecycline upregulated the activating transcription factor 6 (ATF6) levels, both the full length and the cleaved (active) form. This resulted in an increase of the levels of C/EBP homologous protein (DDIT3) (Fig. 3E), which links ER and mitochondrial pathways. On the contrary, 5-FU did not significantly modify the levels of ATF6 or DDIT3 (Fig. 3E) but increased the levels of the phosphorylated and active form of Jun-N-terminal kinase (JNK) (Fig. 3E), which justifies its ability to promote apoptosis through ER pathway. Although tigecycline also increased the levels of phospho-JNK, this was only observed when the p54 isoform was considered, and with a lower efficacy in comparison with 5-FU (Fig. 3E). Moreover, both, tigecycline and 5-FU, significantly increased the ratio between phospho-JUN and JUN (Fig. 3E), thus favoring the activation of this proapoptotic ligand.

3.3. Tigecycline attenuates tumorigenesis in AOM/DSS treated mice

Upon the observation of the in *vitro* anti-tumoral effect of tigecycline, we studied it in vivo. CRC was induced by the well-described AOM/DSS model. As evidenced by colonoscopy, the administration of either tigecycline or 5-FU exerted beneficial effects ameliorating tumoral progression (Fig. 4 A). The tumor score, based on the size of the tumors [31], was significantly reduced in all treated groups in comparison with untreated control mice (Fig. 4 A), as well as the tumor count (Fig. 4B). Thus, both treatments had a positive impact toward reducing tumor number, with a trend to lower the tumor size (Fig. 4B-D and S2A). These observations were supported by the histological analysis, which confirmed the presence of a higher number of adenocarcinomas in non-treated CAC mice than in treated mice (Fig. 4E). Histological staining with anti-MKI67 showed that tigecycline and 5-FU induced a reduction of the proliferation index (Fig. 4F), thus supporting the anti-proliferative impact of both drugs in this model.

We sought to evaluate the molecular mechanisms underlying these effects. We could confirm that the inhibitory actions of tigecycline treatment on CAC progression are mediated by modulation of the Wnt/β-catenin signaling pathway, as observed in the in vitro evaluation. Administration of tigecycline to CAC mice inhibited STAT3 activation in the colon by reducing the ratio of phospho-STAT3/STAT3 (Fig. 4G), and subsequently, ameliorated *Ccnd1* and *Mmp9* expressions, which were upregulated in control mice (Fig. 4G). Moreover, a trend to reduce the colonic expression of CTNNB1 was observed with both doses of tigecycline and 5-FU (Fig. 4G). The treatments also restored the phospho-AKT/AKT ratio, altered by AKT phosphorylation with cancer progression (Fig. 4G), which could reduce the proliferative effects and angiogenesis process through VEGFA and ANGPT2 up-regulation [38]. Thus, in this study, a significant reduction of *Angpt2* gene expression was observed in mice treated with tigecycline versus CAC group (Fig. 4G).

The flow cytometry analysis of isolated colonocytes indicated that AOM/DSS stimulus significantly increased the levels of $LGR5^+$ and $LGR5^+CD44^+$ cancer stem cells (CSC), key drivers of the initiation and progression of the tumoral process. Tigecycline treatment significantly reduced both populations (Fig. 5A). This reduction was confirmed by SNAI1 protein analysis, an EMT process marker involved in the formation of these CSCs [39]. Thus, the treatment with tigecycline reduced the protein levels of SNAI1 compared with the CAC group (Fig. 5B).

Moreover, the anti-tumor effect of tigecycline was also related to a pro-apoptotic impact. By TUNEL assay, we observed an increase of the number of apoptotic cells in mice treated with both tigecycline and 5-FU (Fig. 5C). In line with the in vitro described mechanisms, apoptosis induction with tigecycline treatment involved the increase of CASP7 full length and cleaved levels (Fig. 5D). Moreover, tigecycline and 5-FU treated mice also showed normalized BCL2 levels compared to CAC-mice (Fig. 5D), which contributes to the pro-apoptotic effect.

The inflammatory status of the disease was assessed throughout the induction process by monitoring the DAI (Fig. 6A). 5-FU treatment did not show any statistical differences in comparison with the CAC group at the end of the assay, but tigecycline did reduce DAI value (Fig. 6A). Accordingly, tigecycline lowered the expression of some cytokines involved in the tumor-associated inflammatory response in the colon, like *Tnfa, Il6, Il17a* and *Il23a* (Fig. 6B).

When the impact of the tigecycline on the myeloid populations from colon ($CD45^+CD11b^+$) (Fig. S3) and lymphoid cells MLN ($CD3^+CD4^+$/$CD3^+CD8^+$) (Fig. S4) was analyzed, we observed a reduced infiltration of myeloid cells ($CD45^+CD11b^+$) in the colon (Fig. S3), and similar numbers of $CD3^+CD4^+$ cells among the T cells from MLN in the different groups, but a significant reduction of CTLs in CAC group (Fig. 6C and D). When $CD3^+CD4^+IFN\gamma^+$ (Th1 phenotype) population was considered, the highest dose of tigecycline produced a significant increase (Fig. 6D). Interestingly, this increment has been associated with a protective response against CAC through favoring the recruitment of CTLs [40]. In fact, when CTL population was analyzed, tigecycline and 5-FU increased its level in comparison with non-treated CAC-mice (Fig. 6D), particularly those CTLs with IFNG production (Tc1) (Fig. 6D).

3.4. Tigecycline mitigates CAC by regulating gut microbiota

The 16 S rRNA sequencing results showed an alteration on bacterial composition in AOM/DSS treated mice. Tigecycline 25 mg/kg and 5-FU significantly increased alpha diversity, calculated by different indexes (observed species, Shannon, ACE, and Simpson), in comparison with

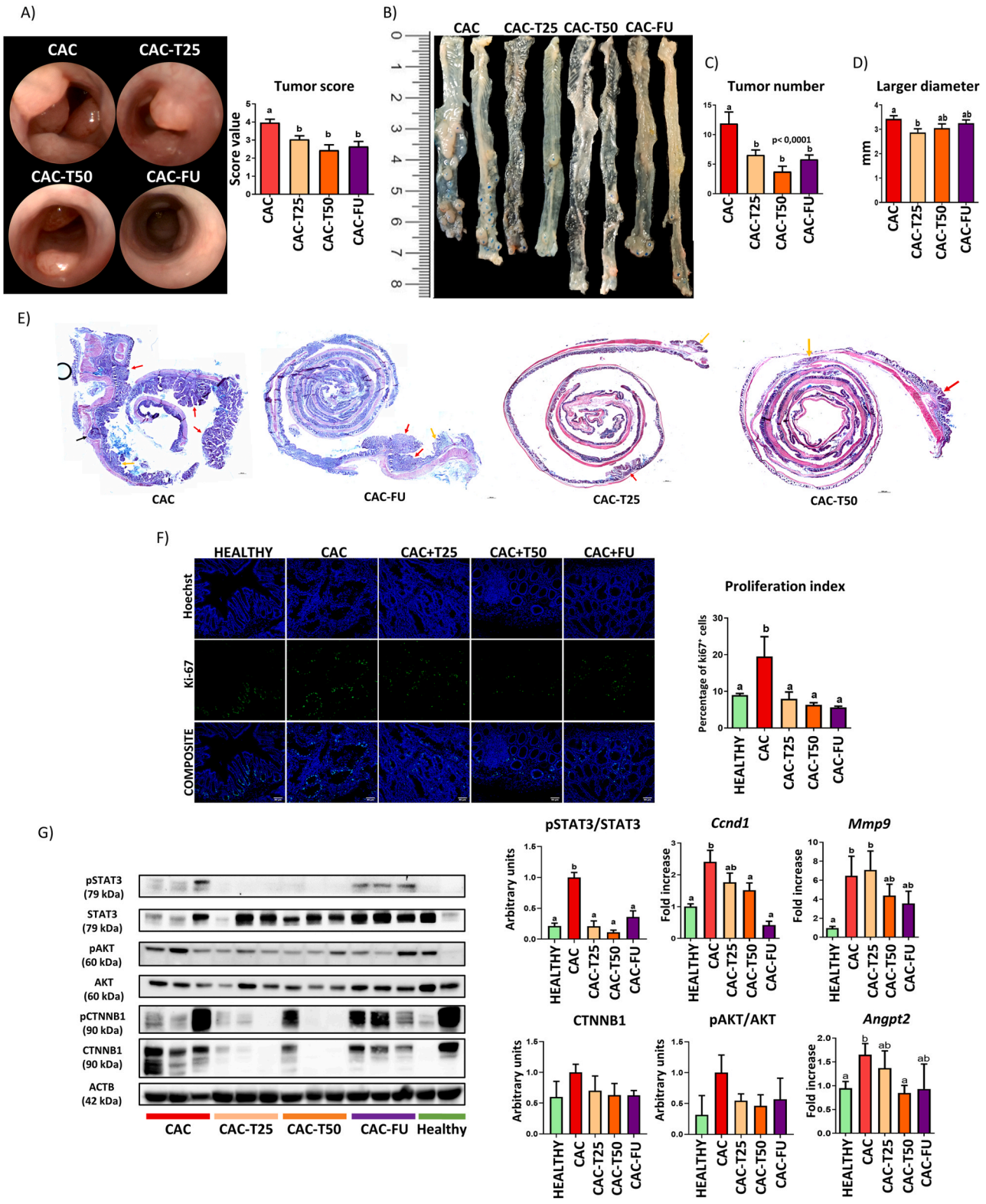

Fig. 4. Impact of tigecycline and 5-FU on tumorigenesis in colonic samples in a CAC (AOM/DSS)mouse model (n = 10). (A) Representative colonoscopy images and tumor score based on the size of the tumor evaluated by colonoscopy (B) Representative colon images of CAC, CAC-T25, CAC-T50 and CAC-FU mice, (C) tumor number and (D) tumor size. (E) Representative images of histological sections of colon. Adenocarcinomas are indicated with red arrows, adenomas with blue arrows and a lymph node with black arrow. Scale bar: 500 μm. (F) Ki67 immunofluorescence staining (green) was conducted to identify actively proliferating cells and proliferation index was calculated from the percentage of ki67-positive cells in ratio to total cells per field. Scale bar: 50 μm (G) Protein levels and gene expression of several markers involved in cell proliferation evaluated and detected in colon. Data are presented as mean ± SEM. Bars with different letter differ statistically ($P < 0.05$).

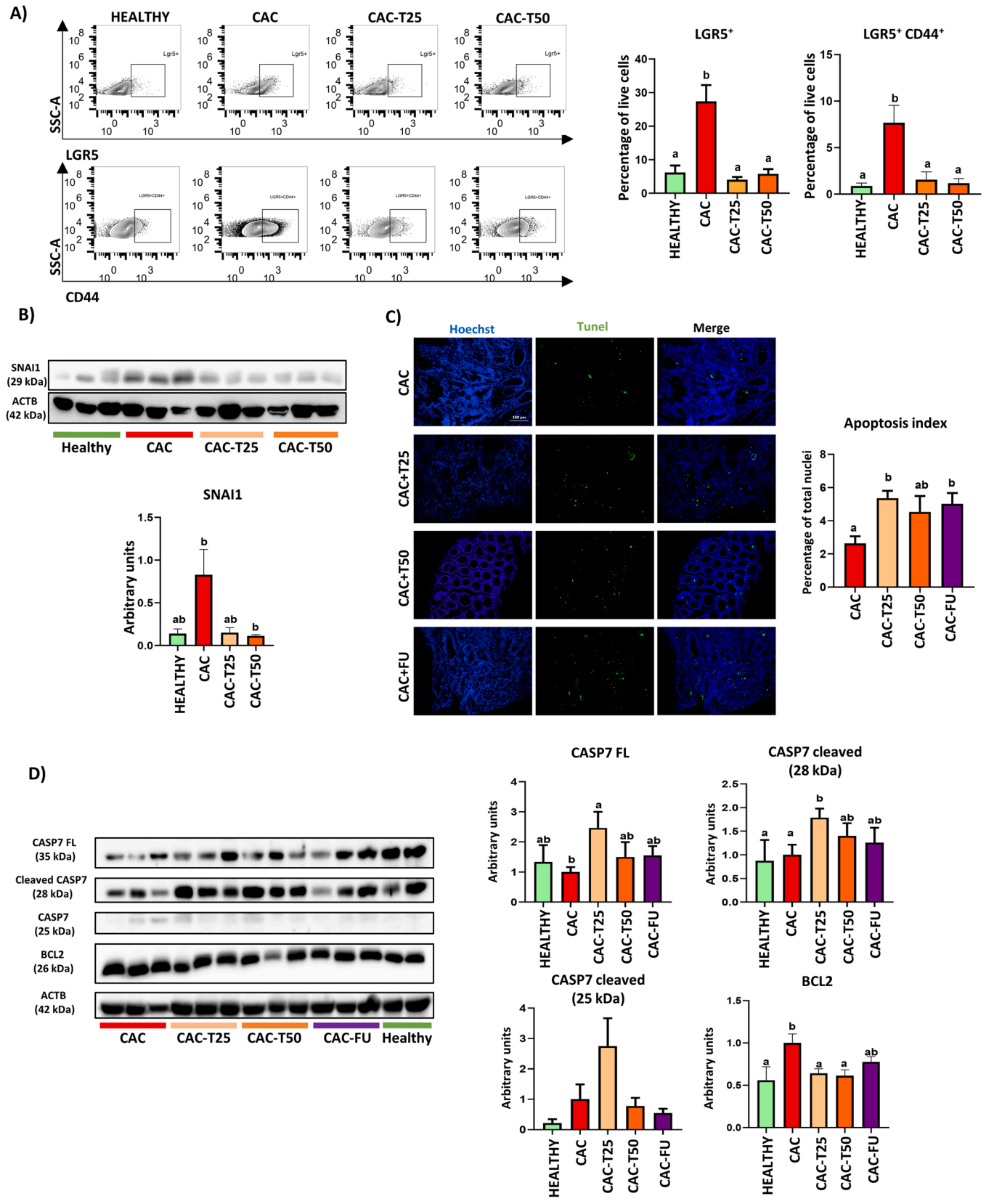

Fig. 5. Impact of tigecycline and 5-FU on stemness and apoptosis in colon samples in CAC mice. (A) Representative flow cytometry analysis of LGR5 + population and quantification of $LGR5^{+}$ and $LGR5^{+}CD44^{+}$ cells populations in each experimental group. (B) Changes in SNAI1 levels induced by the CAC process and tigecycline treatment analyzed by Western blot in colon. (C) Representative fluorescence images of Tunel assay-stained (apoptosis) colonic tissue sections from CAC, CAC-T25, CAC-T50 and CAC-FU mice (n = 4). Apoptotic cells are stained in green and nuclei in blue (Hoechst). The apoptosis index was calculated as $Tunel^{+}$ cells/total cells per field. Scale bar: 100 μm. (D) Levels of several markers involved in apoptosis and cell survival analyzed in colon tissue by Western blot. Data are presented as mean ± SEM. Bars with different letter differ statistically ($P < 0.05$).

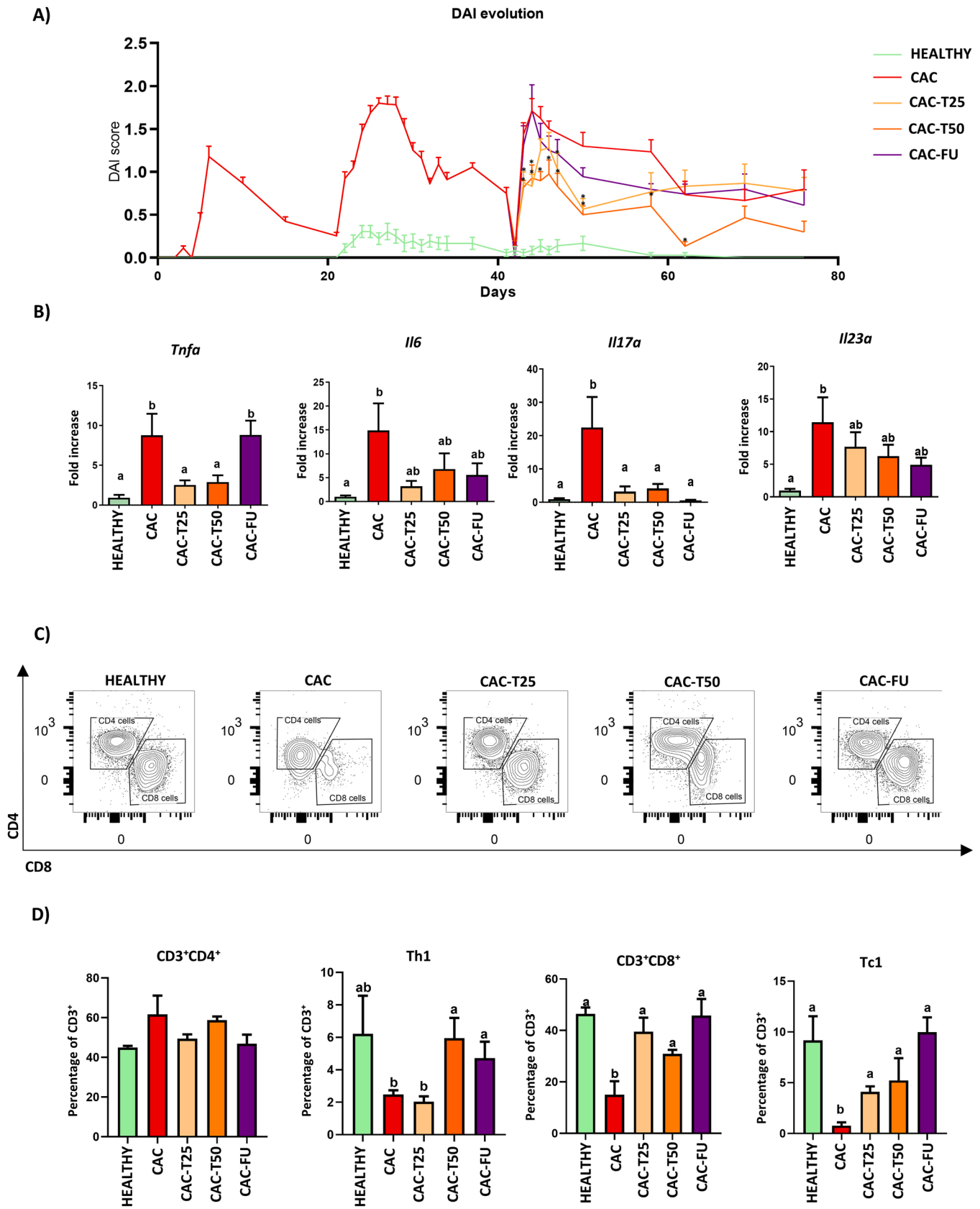

Fig. 6. Effect of tigecycline and 5-FU on CRC-associated inflammation and lymphocytes (CD3 +) populations in mesenteric lymph nodes. (A) DAI score (n = 10). (B) Impact on the cytokines gene expression quantified by real-time qPCR (n = 8). (C) Representative strategy gating dot plots of mesenteric lymph nodes from HEALTHY, CAC, CAC-T25, CAC-T50 and CAC-FU mice (n = 4–5) showing the CD4 vs. CD8 T lymphocyte distribution. (D) CD3 +CD4 + , Th1, CTLs (CD3 +CD8 +) and Tc1 populations levels from mesenteric lymph nodes samples isolated from HEALTHY, CAC, CAC-T25, CAC-T50 and CAC-FU mice. Fold increase was calculated vs. control group. Data are presented as mean ± SEM. Bars with different letter differ statistically ($P < 0.05$).

untreated CAC group (Fig. 7A). Besides, the beta diversity determined by weighted unifrac analysis revealed a clear separation in the Principal Coordinates Analysis (PCoA) between healthy and CAC group, indicating that the homeostasis of gut microbiota was dramatically disrupted by the AOM/DSS stimulus (Fig. 7B). Remarkably, the 5-FU mice and the lowest dose of tigecycline showed more resemblance to the healthy group (Fig. 7B). Consistently, the Venn diagram (prevalence 75%) showed that there were only 4 common OTUs among healthy and CAC groups, and that the highest number of shared OTUs was presented among healthy group and tigecycline group (25 mg/kg, 48 shared OTUs) (Fig. 7C).

The gut microbiota taxa and their abundance were also analyzed. As shown in Fig. 7D, the relative taxonomic composition at the phylum level mainly contained *Bacillota*, *Bacteroidota*, *Pseudomonadota* and *Verrucomicrobiota.* The relative abundance of *Bacillota* and *Actinomycetota* was diminished in the AOM/DSS-induced group in comparison to the control group, while *Bacteroidota*, *Pseudomonadota*, and *Verrucomicrobiota* abundance was increased (Fig. 7D). Notably, the administration of tigecycline mitigated the variation of gut microbiota composition caused by AOM/DSS stimulation (Fig. 7D). Moreover, the *Bacillota/Bacteroidota* (named F/B) ratio in the CAC group was significantly lower than in the control mice, and the administration of the lowest dose of tigecycline was able to significantly increase the ratio compared with CAC mice (Fig. 7E). At genus level, the heatmap showed that some bacteria abundance was increased in the CAC group when compared to healthy mice (*Akkermansia*, *Turicibacter*, *Lachnospiraceae*, *Desulfovibrio* and *Enterorhabdus*) (Fig. 7F). All these genera abundance was restored by the treatment with tigecycline (Fig. 7 F). Conversely, different bacterial genera were reduced in untreated mice compared with the healthy group (*Coriobacteriaceae*, *Lactobacillus*, and *Dubosiella*) (Fig. 7F), and even lower in treated CAC mice (Fig. 7F).

Volcano plots provide us information about the amount of OTUs that are downregulated and upregulated with respect to the control CAC group. Specifically, in healthy and CAC-FU the higher number of OTUs were upregulated, 93 and 130 OTUs, respectively (Fig. 8A). When the Venn diagram was determined with the upregulated OTUs the results showed that none of them were shared between the four groups. Conversely, 1 of them corresponding to *Parabacteroides* genus was observed among the three treated groups (Fig. 8B). Moreover, 6 OTUs were up-regulated and shared among mice treated with the two doses of tigecycline (Fig. 8B): *Enterobacteriaceae* family, *Akkermansia* and *Bacteroides* genera, as well as, *Parabacteroides distasonis* and *uncultured Bacteroidales bacterium* bacterial species (Fig. 8B). On the other hand, in tigecycline-treated mice, the higher number of OTUs were found downregulated: 87 and 130 OTUs, respectively (Fig. 8B). 3 of them were significantly downregulated and shared in the three groups of treated mice: *Dubosiella* genus and *Dubosiella newyorkinensis* and *Clostridium sp. ASF502* bacterial species (Fig. 8B). When tigecycline treated groups were compared only two bacterial genera (*Faecalibaculum* and *A2* from *Lachnospiraceae)* were decreased and shared (Fig. 8B).

Focusing on OTUs shared from treated and healthy mice, *Ruminococcus 1* and *Erysipelatoclostridium* genera, *Lachnospiraceae bacterium* COE1 and *Clostridium* sp. Clone-47 species were found down-regulated in healthy, CAC-T50 and CAC-FU groups (Fig. 8B). Additionally, the genus *Ruminococcaceae* UCG-013 was decreased in healthy and tigecycline 50 mg/kg treated mice (Fig. 8B).

Finally, the heat map constructed with data from control CAC mice and tigecycline treated mice showed a positive correlation between the relative abundance of *Akkermansia* and *P. distasonis* and parameters that indicates a good prognosis of the disease such as CTLs levels, fewer number of tumors and levels of inflammation and proliferation markers (Fig. 8C).

4. Discussion

CRC incidence and mortality rates are still high, so the development of novel therapeutic strategies is necessary. In this study, we demonstrated the effectiveness of tigecycline in the treatment of CRC in vitro and in a murine model of CAC. Moreover, our findings provide the first evidence that tigecycline exerts an anti-proliferative and pro-apoptotic effect, as well as immunomodulatory properties and the ability to modulate gut dysbiosis in CRC.

This study agrees with and supports previous studies that have deemed some antibiotics as promising candidates for cancer therapy [41]. In fact, different antibiotic drugs, including tigecycline, have been recently reported to impact growth of various types of tumor cells and show positive therapeutic effects in cancer patients [42]. The antitumor mechanisms of tigecycline remain unidentified, but one of them could be the capacity of tigecycline to regulate cell proliferation rate. In fact, previous studies have showed that tigecycline exerts a direct inhibitory effect on TLR-dependent monocyte/macrophage responses [43] as well as antitumoral activity by targeting specific rRNA substructures, activation of the ISR, and inhibition of translation in human cancer cell lines [44]. Moreover, several studies have proposed the ability of some tetracyclines, like doxycycline and minocycline, to inhibit matrix metalloproteinases (MMPs) and/or DNA-dependent protein kinase activities [23].

Additionally, almost 80% of CRC patients [4] show mutations in APC gene which lead to alterations on Wnt/β-catenin signaling pathway. Thus, CTNNB1 aberrant activation and nuclear translocation boost the expression of oncogenes involved in cell cycle and proliferation such as *AXIN2, MYC* and *CCND1* [5], increasing cell proliferation and promoting the tumorigenesis process, including migration, invasion, apoptosis evasion and chemoresistance [45]. The present study demonstrates that tigecycline suppressed tumorigenesis by downregulating the Wnt/β-catenin signaling pathway, confirming previous studies in cervical squamous cell carcinoma [42]. Additionally, we also show that tigecycline can enhance the phosphorylation of CTNNB1 in tumor cells, even when the Wnt/β-catenin pathway is overstimulated with Wnt3a ligand. This action increases the degradation of CTNNB1 downregulating the expression of genes such as *AXIN2* and *MYC*.

Other signaling pathways are also altered in the tumoral process, including JAK/STAT3 and PI3K/AKT/mTOR. These pathways are involved in the proliferation, survival, and metastasis of CRC, as well as immune and apoptosis evasion and poor patient outcomes [46,47]. In this regard, there is evidence that STAT3 signaling contributes to the stimulation of *CCND1* and *MYC* expression promoting cell-cycle progression and proliferation [47]. Besides, STAT3 favors cell survival and invasion through the up-regulation of *Bcl2* and *Mmp9* [48,49]. Accordingly, we found that tigecycline treatment decreased the expression of these markers, which could explain its capacity to inhibit STAT3 activation. Other antibiotics have also displayed antitumor effects through the inhibition of STAT3 in different types of cancer [49].

In addition, it has been demonstrated that individual CRCs contain cells at various stages of differentiation, with cancer stem cells (CSCs) driving tumor growth and progression. Many studies have confirmed that CSC initiate the tumor process and are the main responsible for resistances to treatment and recurrences in CRC [50]. CSCs display survival mechanisms as apoptosis evasion or the capability to establish quiescent state, thus circumventing conventional antineoplastic treatments. In this regard, tigecycline interferes with the generation of CSCs, reducing the population of $LGR5^{+}CD44^{+}$ cells. Our findings have clinical relevance since tigecycline could be considered for conducting future clinical trials on the treatment of CRC, including “pre-malignant” and advanced metastatic process. Supporting this finding, tigecycline has previously shown capacity to eradicate CSC across different tumor types (breast, ductal carcinoma in situ, ovarian, prostate, lung, pancreatic, melanoma, and glioblastoma) [51], maybe mediated by mitochondrial inhibition.

Additionally, EMT process is crucial for CSC generation and, therefore, for the development and progression of CRC [52]. Tigecycline has shown that interferes with the expression of SNAI1, a marker involved in

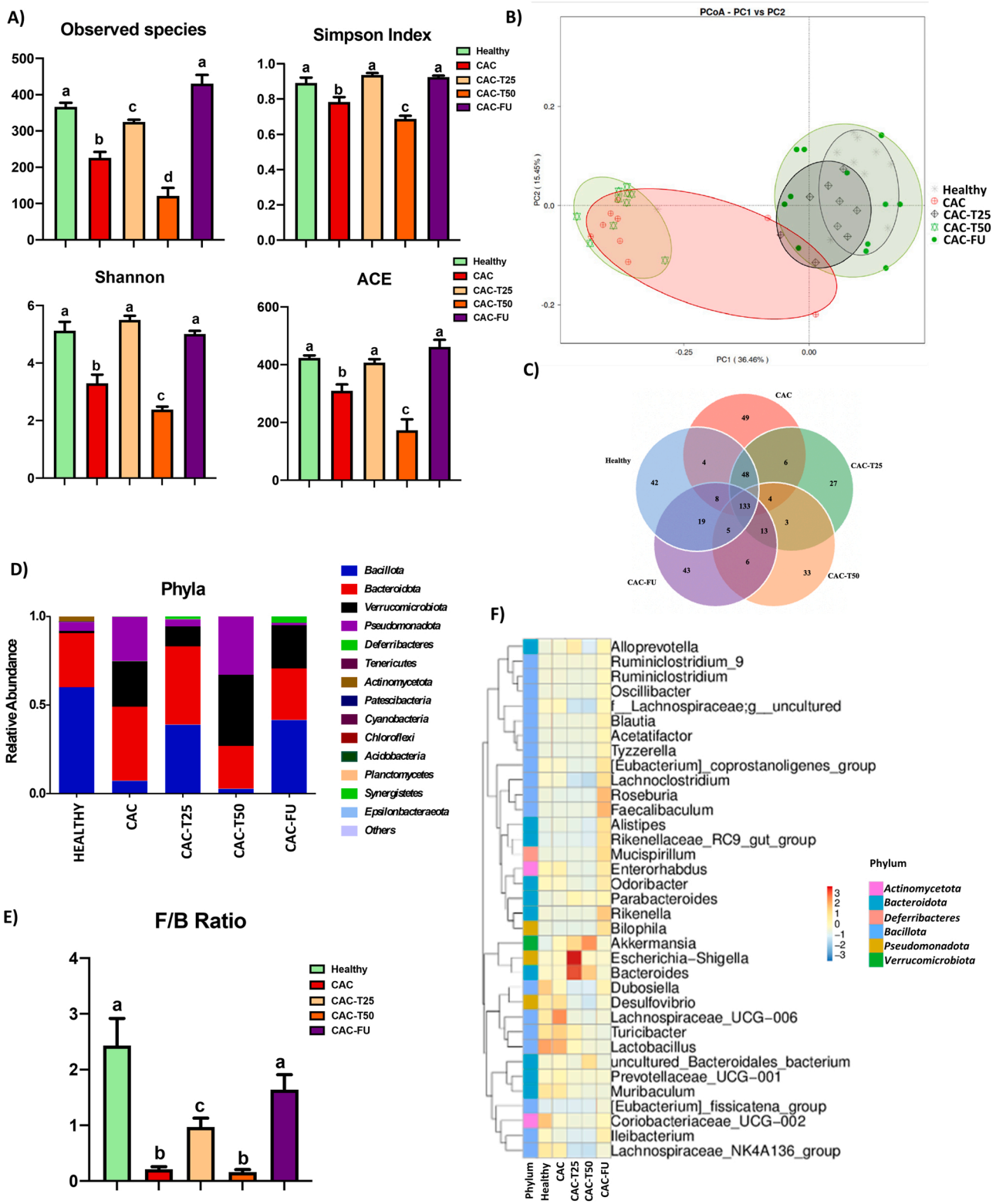

Fig. 7. Effect of tigecycline and 5-FU on gut microbiota composition (n = 9). (A) Microbiome diversity indexes calculated after faecal microbiota Illumina sequencing: observed species, Simpson index, Shannon index and ACE index. (B) β-diversity by principal coordinate analysis score plot. (C) A Venn diagram showing the number of OTUs which are unique and common to each experimental group. (D) Distribution histogram of relative abundance of taxa. (E) *Bacillota/Bateroidota* (named F/B) ratio in each experimental group (F) A heatmap showing the taxonomic signatures at the genus level. Data are presented as mean ± SEM. Bars with different letter differ statistically ($P < 0.05$).

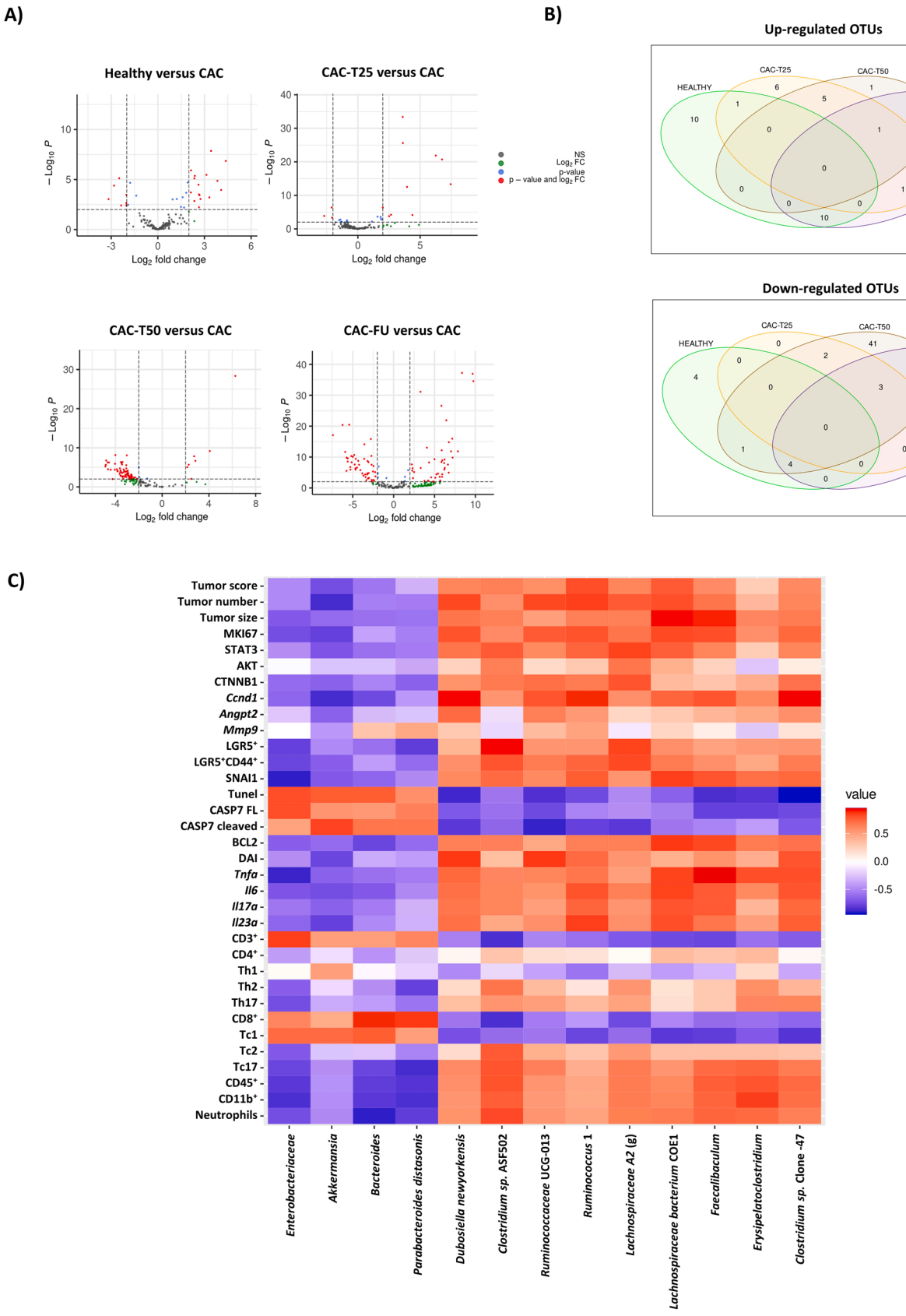

Fig. 8. Effect of tigecycline and 5-FU on gut microbiota composition and correlation between bacterial abundance and functional features in each group (n = 9). (A) Volcano plot indicating the upregulated and downregulated OTUs in Healthy, CAC-T25, CAC-T50 and CAC-FU in comparison with those OTUs determined on CAC group. (B) Venn-diagrams that show the down-regulated shared OTUs and the up-regulated shared OTUs between Healthy, CAC-T25, CAC-T50 and CAC-FU when compared with CAC group. (C) Heat-map of correlations between gut microbiota changes and different features analyzed in vivo between tigecycline-treated mice and untreated-CAC mice.

the EMT process, in this study, and earlier, in melanoma [53].

As it is widely known, evasion of cell death is one of the hallmarks of cancer. Previous studies have evidenced that tetracyclines can induce apoptosis in different cell lines, including tumor cells [54]. Our findings corroborate these results and, also, demonstrate the apoptotic activity of tigecycline in vitro and in vivo. Interestingly, molecular mechanisms involved in tigecycline-mediated apoptosis are different from those displayed by 5-FU. The latest activates intrinsic apoptosis through TP53 upregulation, whereas tigecycline exerts its action downstream, at BAX level. Moreover, our findings support that CASP3 and CASP7 are the main apoptosis executioners in 5-FU treatment, whereas CASP7 is involved in the tigecycline-mediated apoptosis. In any case, both treatments lead to PARP1 cleavage and cell death. This action is shared by different anticancer drugs, such as etoposide, being considered as an early marker of chemotherapy-induced apoptosis [55].

We also show that both treatments target ER-mediated apoptosis markers, favoring the induction of cell death through this pathway. 5-FU increased the ER-mediated apoptosis through the activation of the two isoforms of JNK. Tigecycline also acts at this level, however, it only favors the activation of p54 isoform, which, according to Waetzig V et al., 2003, is enough for taxol-mediated apoptosis [56]. Dissimilar to 5-FU, tigecycline also activates this pathway through its action on ATF6.

Besides, as previously commented, the tumor microenvironment has an essential role in tumor progression and prognosis. Thus, chronic inflammatory stimuli triggers cancer initiation and progression, as occurs in this experimental CAC model, and IBD patients, who have an increased risk of developing CRC [7]. On the other hand, the immune system also plays an important role attacking the tumor cells. In CRC, altered Th1/Th2 response contributes to tumor progression, while enhanced Th1 population is associated with better prognosis [57]. Furthermore, CTLs are the preferred immune cells for tumor surveillance and are the most powerful effectors in immune cancer targeting [58]. Accordingly, we showed that the development of CAC was associated with a depletion of T cells, specifically CTLs in the colon of non-treated CAC mice. However, the treatment with tigecycline and 5-FU restored CTL levels. In fact, 5-FU and the lowest dose of tigecycline, significantly increased Tc1 cells, which plays an important role in the antitumor effect of these lymphocytes, being IFNγ producers and considered an indicator of CTL activation [40].

Finally, it is well accepted that alterations in gut microbiota composition contributes to tumor development and are associated with CRC [8,9]. Although it is not clear whether dysbiotic changes have a causal role or follow environmental changes produced by tumor onset, there is enough evidence supporting the role of certain bacteria in cancer initiation and progression as well as cancer protection [8,9]. Therefore, modulation of this altered microbiota in CRC with drugs such as antibiotics, could be considered a complementary therapeutic approach [11]. Correspondingly, our results confirm the existence of a dysbiotic status in the CAC group characterized by a reduced microbial diversity, as seen before [59], while the lower dose of tigecycline restored this microbial diversity. Supporting the clinical importance of the latest, other antibiotics, including tetracyclines, have shown the ability to modulate the dysbiosis in oncology patients [60].

Over the last decade, several bacteria species have gained interest for their involvement in colorectal carcinogenesis [8]. *Akkermansia muciniphila* stands out among these species for its anti-inflammatory and protective functions on gut barrier [61]. The relationship between *A. muciniphila* and CRC remains controversial. Different studies have shown an enrichment of *Akkermansia* in CRC patients [62], while others have reported that it can mitigate tumorigenesis in CRC with capacity to boost the effect of existing antitumor treatments [63]. In this study we observed an increase in *Akkermansia* genus in CAC mice compared to healthy mice, as well as increased levels in mice treated with tigecycline, which may contribute to its beneficial effect. Additionally, *P. distasonis* is a gram-negative anaerobic bacterium that has been associated with an attenuation of tumorigenesis and inflammation by interfering production of cytokines and proliferation mediators, such as AKT [64]. Tigecycline treatment increased levels of *P. distasonis*, which can be related to the modulation of the inflammatory markers and the promotion of the intestinal barrier integrity, as reported previously in other studies [64]. Indeed, the correlation analysis showed a negative association between *Akkermansia* genus and *P. distasonis* and some macroscopic parameters such as tumor number, size and DAI, as well as molecular markers of proliferation (STAT3, CTNNB1 and *Ccnd1* gene expression), survival (BCL2), stemness (SNAI1) or inflammation (*Il6, Il17a, Il23a, Tnfa* gene expression). Moreover, *Akkermansia* sp. and *P. distasonis* abundance are positively correlated with apoptosis (Tunel and CASP7) and cytotoxic activity (CTLs and Tc1 response) (Fig. 8 C). Consequently, the connection between both bacteria species can contribute to tumorigenesis attenuation.

Human colonic microbiota can process a wide range of substrates that escape digestion by the host. Among *Bacillota*, the *Lachnospiraceae* and *Ruminococcaceae* species hydrolyze starch and other sugars to produce butyrate and other short chain fatty acids (SCFAs). Initially, these SCFA-producing species have been associated with an improvement of the outcomes in different clinical settings including CRC and IBD [65]. Despite this, other studies have reported an increase in *Lachnospiraceae* and *Ruminococcus* genera in CRC patients [66]. Here, we found down-regulation of *Ruminococcus* and *Lachnospiraceae* species in healthy and treated groups when compared with control CAC.

On the other hand, bacterial species from the *Erysipelatoclostridium* genus, such as *E. ruminantium* and *E. ramosum,* have been reported to be increased in adenoma [67]. In this regard, we found a lower abundance of *Erysipelatoclostridium* in both, healthy and tigecycline treated groups. Indeed, in this study we show a positive correlation between tumor size and markers associated with tumor progression and the abundance of *Ruminococcaceae* UCG-013*, Ruminococcus 1, Lachnospiraceae A2, Lachnospiraceae bacterium* COE1 and *Erysipelatoclostridium* (Fig. 8 C).

In conclusion, this study has demonstrated the capacity of tigecycline to induce a sustained attenuation of tumorigenesis in CRC, evidenced by a reduced tumor number and characterized by reduction of tumor cells proliferation, induction of apoptosis, as well as amelioration of inflammation and modulation of gut dysbiosis. Therefore, our data support the treatment with tigecycline as a novel therapeutic strategy against CRC.

Funding statement

This work was funded by the Junta de Andalucía (CTS 164); the Instituto de Salud Carlos III (Spain) and Fondo Europeo de Desarrollo Regional (FEDER), from the European Union, through the research grants PI18/00826, P18-RT-4930, PI0206–2016, PIE16/00045 and PI19/01058; Spanish Ministry of Science and Innovation (MCIN/AEI/10.13039/501100011033/FEDER) under grant RTI2018–101309-B-C22; and the Chair "Doctors Galera-Requena in cancer stem cell research" (CMC-CTS963). A.J. R-M L. H-G are predoctoral fellows funded by the Spanish Ministry of Science and Innovation ("Programa de Doctorado: Medicina Clínica y Salud Pública" B12.56.1). M.J. R-S and J. A. M-T are predoctoral fellows from the Instituto de Salud Carlos III (FI17/00176). P. D-E is a postdoctoral fellow of Junta de Andalucía (P18-RT-4930). T. V and J. G-M are postdoctoral fellows from the University of Granada. CIBER-EHD is funded by the Instituto de Salud Carlos III.

CRediT authorship contribution statement

All authors performed the experiments and contributed to the acquisition. Federico García, Antonio Jesús Ruiz-Malagón and Alba Rodríguez-Nogales carried out the microbiome studies. Antonio Jesús Ruiz-Malagón, María Elena Rodríguez-Cabezas, Alba Rodríguez-Nogales and José Garrido-Mesa designed the experiments. All authors drafted the manuscript, read, and approved the final manuscript.

Conflict of interest statement

The authors have declared no conflicting interests.

Data availability

Data will be made available on request.

Appendix A. Supporting information

Supplementary data associated with this article can be found in the online version at doi:10.1016/j.biopha.2023.114760.

References

[1] Y.H. Xie, Y.X. Chen, J.Y. Fang, Comprehensive review of targeted therapy for colorectal cancer, Signal Transduct. Target Ther. 5 (2020) 22, https://doi.org/10.1038/s41392-020-0116-z.

[2] J.M. Carethers, B.H. Jung, Genetics and genetic biomarkers in sporadic colorectal cancer, e1173, Gastroenterology 149 (2015) 1177–1190, https://doi.org/10.1053/j.gastro.2015.06.047.

[3] E.R. Fearon, B. Vogelstein, A genetic model for colorectal tumorigenesis, Cell 61 (1990) 759–767, https://doi.org/10.1016/0092-8674(90)90186-I.

[4] V. Korinek, N. Barker, P.J. Morin, D. van Wichen, R. de Weger, K.W. Kinzler, B. Vogelstein, H. Clevers, Constitutive transcriptional activation by a beta-catenin-Tcf complex in APC-/- colon carcinoma, Science 275 (1997) 1784–1787, https://doi.org/10.1126/science.275.5307.1784.

[5] S. Shang, F. Hua, Z.W. Hu, The regulation of beta-catenin activity and function in cancer: therapeutic opportunities, Oncotarget 8 (2017) 33972–33989, https://doi.org/10.18632/oncotarget.15687.

[6] J. Terzic, S. Grivennikov, E. Karin, M. Karin, Inflammation and colon cancer, e2105, Gastroenterology 138 (2010) 2101–2114, https://doi.org/10.1053/j.gastro.2010.01.058.

[7] W.T. Clarke, J.D. Feuerstein, Colorectal cancer surveillance in inflammatory bowel disease: Practice guidelines and recent developments, World J. Gastroenterol. 25 (2019) 4148–4157, https://doi.org/10.3748/wjg.v25.i30.4148.

[8] W.S. Garrett, The gut microbiota and colon cancer, Science 364 (2019) 1133–1135, https://doi.org/10.1126/science.aaw2367.

[9] H. Tjalsma, A. Boleij, J.R. Marchesi, B.E. Dutilh, A bacterial driver-passenger model for colorectal cancer: beyond the usual suspects, Nat. Rev. Microbiol 10 (2012) 575–582, https://doi.org/10.1038/nrmicro2819.

[10] M. Lopez-Siles, M. Martinez-Medina, R. Suris-Valls, X. Aldeguer, M. Sabat-Mir, S. H. Duncan, H.J. Flint, L.J. Garcia-Gil, Changes in the Abundance of Faecalibacterium prausnitzii Phylogroups I and II in the Intestinal Mucosa of Inflammatory Bowel Disease and Patients with Colorectal Cancer, Inflamm. Bowel Dis. 22 (2016) 28–41, https://doi.org/10.1097/MIB.0000000000000590.

[11] W. Fong, Q. Li, J. Yu, Gut microbiota modulation: a novel strategy for prevention and treatment of colorectal cancer, Oncogene 39 (2020) 4925–4943, https://doi.org/10.1038/s41388-020-1341-1.

[12] J. Garrido-Mesa, A. Rodriguez-Nogales, F. Algieri, T. Vezza, L. Hidalgo-Garcia, M. Garrido-Barros, M.P. Utrilla, F. Garcia, N. Chueca, M.E. Rodriguez-Cabezas, et al., Immunomodulatory tetracyclines shape the intestinal inflammatory response inducing mucosal healing and resolution, Br. J. Pharm. 175 (2018) 4353–4370, https://doi.org/10.1111/bph.14494.

[13] A.M. Kroon, B.H.J. Dontje, M. Holtrop, C. Van Den Bogert, The mitochondrial genetic system as a target for chemotherapy: Tetracyclines as cytostatics, Cancer Lett. 25 (1984) 33–40, https://doi.org/10.1016/S0304-3835(84)80023-3.

[14] Z. Saikali, G. Singh, Doxycycline and other tetracyclines in the treatment of bone metastasis, Anti-Cancer Drugs 14 (2003) 773–778, https://doi.org/10.1097/01.cad.0000099002.92896.cf.

[15] L. Sanchez-Burgos, B. Navarro-Gonzalez, S. Garcia-Martin, O. Sirozh, J. Mota-Pino, E. Fueyo-Marcos, H. Tejero, M.E. Anton, M. Murga, F. Al-Shahrour, et al., Activation of the integrated stress response is a vulnerability for multidrug-resistant FBXW7-deficient cells, EMBO Mol. Med 14 (2022), e15855, https://doi.org/10.15252/emmm.202215855.

[16] Y. Zhou, S. Wang, W. Wu, J. Ling, H. Li, Q. Jia, J. Zheng, X. Zheng, R. Yu, Q. Wu, et al., Sustained activation of EGFR-ERK1/2 signaling limits the response to tigecycline-induced mitochondrial respiratory deficiency in liver cancer, EBioMedicine 87 (2023), 104397, https://doi.org/10.1016/j.ebiom.2022.104397.

[17] M.H. Pourgholami, A.H. Mekkawy, S. Badar, D.L. Morris, Minocycline inhibits growth of epithelial ovarian cancer, Gynecol. Oncol. 125 (2012) 433–440, https://doi.org/10.1016/j.ygyno.2012.01.006.

[18] H. Song, M. Fares, K.R. Maguire, A. Siden, Z. Potacova, Cytotoxic effects of tetracycline analogues (doxycycline, minocycline and COL-3) in acute myeloid leukemia HL-60 cells, PLoS One 9 (2014), e114457, https://doi.org/10.1371/journal.pone.0114457.

[19] M.O. Griffin, G. Ceballos, F.J. Villarreal, Tetracycline compounds with non-antimicrobial organ protective properties: possible mechanisms of action, Pharm. Res 63 (2011) 102–107, https://doi.org/10.1016/j.phrs.2010.10.004.

[20] G.N. Smith Jr, E.A. Mickler, K.A. Hasty, K.D. Brandt, Specificity of inhibition of matrix metalloproteinase activity by doxycycline: Relationship to structure of the enzyme. *Arthritis &*, Rheumatism 42 (1999) 1140–1146, https://doi.org/10.1002/1529-0131(199906)42:6<1140::Aid-anr10>3.0.Co;2-7.

[21] C. Guerin, J. Laterra, T. Masnyk, L.M. Golub, H. Brem, Selective endothelial growth inhibition by tetracyclines that inhibit collagenase, Biochem Biophys. Res Commun. 188 (1992) 740–745, https://doi.org/10.1016/0006-291x(92)91118-a.

[22] C.H. Li, P.L. Liao, Y.T. Yang, S.H. Huang, C.H. Lin, Y.W. Cheng, J.J. Kang, Minocycline accelerates hypoxia-inducible factor-1 alpha degradation and inhibits hypoxia-induced neovasculogenesis through prolyl hydroxylase, von Hippel-Lindau-dependent pathway, Arch. Toxicol. 88 (2014) 659–671, https://doi.org/10.1007/s00204-013-1175-5.

[23] I. Ali, K.O. Alfarouk, S.J. Reshkin, M.E. Ibrahim, Doxycycline as potential anti-cancer agent, Anticancer Agents Med Chem. 17 (2017) 1617–1623, https://doi.org/10.2174/1871520617666170213111951.

[24] M. Antoszczak, A. Markowska, J. Markowska, A. Huczynski, Old wine in new bottles: Drug repurposing in oncology, Eur. J. Pharm. 866 (2020), 172784, https://doi.org/10.1016/j.ejphar.2019.172784.

[25] J. Yang, Z. Dong, A. Ren, G. Fu, K. Zhang, C. Li, X. Wang, H. Cui, Antibiotic tigecycline inhibits cell proliferation, migration and invasion via down-regulating CCNE2 in pancreatic ductal adenocarcinoma, J. Cell Mol. Med 24 (2020) 4245–4260, https://doi.org/10.1111/jcmm.15086.

[26] J. Sun, G. Li, Y. Liu, M. Ma, K. Song, H. Li, D. Zhu, X. Tang, J. Kong, X. Yuan, Targeting histone deacetylase SIRT1 selectively eradicates EGFR TKI-resistant cancer stem cells via regulation of mitochondrial oxidative phosphorylation in lung adenocarcinoma, Neoplasia 22 (2020) 33–46, https://doi.org/10.1016/j.neo.2019.10.006.

[27] Z. Saikali, G. Singh, Doxycycline and other tetracyclines in the treatment of bone metastasis, Anticancer Drugs 14 (2003) 773–778, https://doi.org/10.1097/00001813-200311000-00001.

[28] K.S. Kechagias, S. Chorepsima, N.A. Triarides, M.E. Falagas, Tigecycline for the treatment of patients with Clostridium difficile infection: an update of the clinical evidence, Eur. J. Clin. Microbiol Infect. Dis. 39 (2020) 1053–1058, https://doi.org/10.1007/s10096-019-03756-z.

[29] R. Ma, Y. Zhang, W. Wang, J. Wu, Q. Yang, W. Xu, S. Jiang, Y. Han, K. Yu, S. Zhang, Inhibition of autophagy enhances the antitumour activity of tigecycline in multiple myeloma, J. Cell Mol. Med 22 (2018) 5955–5963, https://doi.org/10.1111/jcmm.13865.

[30] D. Camuesco, M.E. Rodriguez-Cabezas, N. Garrido-Mesa, M. Cueto-Sola, E. Bailon, M. Comalada, B. Arribas, M. Merlos, D. Balsa, A. Zarzuelo, et al., The intestinal anti-inflammatory effect of dersalazine sodium is related to a down-regulation in IL-17 production in experimental models of rodent colitis, Br. J. Pharm. 165 (2012) 729–740, https://doi.org/10.1111/j.1476-5381.2011.01598.x.

[31] C. Becker, M.C. Fantini, M.F. Neurath, High resolution colonoscopy in live mice, Nat. Protoc. 1 (2006) 2900–2904, https://doi.org/10.1038/nprot.2006.446.

[32] A. Dhariwal, J. Chong, S. Habib, I.L. King, L.B. Agellon, J. Xia, MicrobiomeAnalyst: a web-based tool for comprehensive statistical, visual and meta-analysis of microbiome data, Nucleic Acids Res 45 (2017) W180–W188, https://doi.org/10.1093/nar/gkx295.

[33] M.I. Love, W. Huber, S. Anders, Moderated estimation of fold change and dispersion for RNA-seq data with DESeq2, Genome Biol. 15 (2014) 550, https://doi.org/10.1186/s13059-014-0550-8.

[34] M. Zhang, W. Weng, Q. Zhang, Y. Wu, S. Ni, C. Tan, M. Xu, H. Sun, C. Liu, P. Wei, et al., The lncRNA NEAT1 activates Wnt/beta-catenin signaling and promotes colorectal cancer progression via interacting with DDX5, J. Hematol. Oncol. 11 (2018) 113, https://doi.org/10.1186/s13045-018-0656-7.

[35] M. Kawada, H. Seno, Y. Uenoyama, T. Sawabu, N. Kanda, H. Fukui, Y. Shimahara, T. Chiba, Signal transducers and activators of transcription 3 activation is involved in nuclear accumulation of beta-catenin in colorectal cancer, Cancer Res 66 (2006) 2913–2917, https://doi.org/10.1158/0008-5472.CAN-05-3460.

[36] H. Li, H. Zhu, C.-j Xu, J. Yuan, Cleavage of BID by Caspase 8 Mediates the Mitochondrial Damage in the Fas Pathway of Apoptosis, Cell 94 (1998) 491–501, https://doi.org/10.1016/S0092-8674(00)81590-1.

[37] H. Kalkavan, D.R. Green, MOMP, cell suicide as a BCL-2 family business, Cell Death Differ. 25 (2018) 46–55, https://doi.org/10.1038/cdd.2017.179.

[38] S. Revathidevi, A.K. Munirajan, Akt in cancer: Mediator and more, Semin Cancer Biol. 59 (2019) 80–91, https://doi.org/10.1016/j.semcancer.2019.06.002.

[39] W. Zhou, R. Lv, W. Qi, D. Wu, Y. Xu, W. Liu, Y. Mou, L. Wang, Snail contributes to the maintenance of stem cell-like phenotype cells in human pancreatic cancer, PLoS One 9 (2014), e87409, https://doi.org/10.1371/journal.pone.0087409.

[40] P. Bhat, G. Leggatt, N. Waterhouse, I.H. Frazer, Interferon-gamma derived from cytotoxic lymphocytes directly enhances their motility and cytotoxicity, Cell Death Dis. 8 (2017), e2836, https://doi.org/10.1038/cddis.2017.67.

[41] S. Sen, R. Carmagnani Pestana, K. Hess, G.M. Viola, V. Subbiah, Impact of antibiotic use on survival in patients with advanced cancers treated on immune checkpoint inhibitor phase I clinical trials, Ann. Oncol. 29 (2018) 2396–2398, https://doi.org/10.1093/annonc/mdy453.

[42] H. Li, S. Jiao, X. Li, H. Banu, S. Hamal, X. Wang, Therapeutic effects of antibiotic drug tigecycline against cervical squamous cell carcinoma by inhibiting Wnt/beta-catenin signaling, Biochem Biophys. Res Commun. 467 (2015) 14–20, https://doi.org/10.1016/j.bbrc.2015.09.140.

[43] L. Silva Lagos, T.V. Luu, B. De Haan, M. Faas, P. De Vos, TLR2 and TLR4 activity in monocytes and macrophages after exposure to amoxicillin, ciprofloxacin, doxycycline and erythromycin, J. Antimicrob. Chemother. 77 (2022) 2972–2983, https://doi.org/10.1093/jac/dkac254.

[44] J.D. Mortison, M. Schenone, J.A. Myers, Z. Zhang, L. Chen, C. Ciarlo, E. Comer, S. K. Natchiar, S.A. Carr, B.P. Klaholz, et al., Tetracyclines Modify Translation by

Targeting Key Human rRNA Substructures, e1513, Cell Chem. Biol. 25 (2018) 1506–1518, https://doi.org/10.1016/j.chembiol.2018.09.010.
[45] S.P. Tenbaum, P. Ordonez-Moran, I. Puig, I. Chicote, O. Arques, S. Landolfi, Y. Fernandez, J.R. Herance, J.D. Gispert, L. Mendizabal, et al., beta-catenin confers resistance to PI3K and AKT inhibitors and subverts FOXO3a to promote metastasis in colon cancer, Nat. Med 18 (2012) 892–901, https://doi.org/10.1038/nm.2772.
[46] K. Malinowsky, U. Nitsche, K.P. Janssen, F.G. Bader, C. Spath, E. Drecoll, G. Keller, H. Hofler, J. Slotta-Huspenina, K.F. Becker, Activation of the PI3K/AKT pathway correlates with prognosis in stage II colon cancer, Br. J. Cancer 110 (2014) 2081–2089, https://doi.org/10.1038/bjc.2014.100.
[47] J. Luo, R. Yan, X. He, J. He, Constitutive activation of STAT3 and cyclin D1 overexpression contribute to proliferation, migration and invasion in gastric cancer cells, Am. J. Transl. Res 9 (2017) 5671–5677.
[48] H. Xiong, Z.G. Zhang, X.Q. Tian, D.F. Sun, Q.C. Liang, Y.J. Zhang, R. Lu, Y.X. Chen, J.Y. Fang, Inhibition of JAK1, 2/STAT3 signaling induces apoptosis, cell cycle arrest, and reduces tumor cell invasion in colorectal cancer cells, Neoplasia 10 (2008) 287–297, https://doi.org/10.1593/neo.07971.
[49] R. Lu, Y.G. Zhang, J. Sun, STAT3 activation in infection and infection-associated cancer, Mol. Cell Endocrinol. 451 (2017) 80–87, https://doi.org/10.1016/j.mce.2017.02.023.
[50] P.K. Das, F. Islam, A.K. Lam, The roles of cancer stem cells and therapy resistance in colorectal carcinoma, Cells (2020) *9*, https://doi.org/10.3390/cells9061392.
[51] R. Lamb, B. Ozsvari, C.L. Lisanti, H.B. Tanowitz, A. Howell, U.E. Martinez-Outschoorn, F. Sotgia, M.P. Lisanti, Antibiotics that target mitochondria effectively eradicate cancer stem cells, across multiple tumor types: treating cancer like an infectious disease, Oncotarget 6 (2015) 4569–4584, https://doi.org/10.18632/oncotarget.3174.
[52] A. Dongre, R.A. Weinberg, New insights into the mechanisms of epithelial-mesenchymal transition and implications for cancer, Nat. Rev. Mol. Cell Biol. 20 (2019) 69–84, https://doi.org/10.1038/s41580-018-0080-4.
[53] H. Hu, Z. Dong, P. Tan, Y. Zhang, L. Liu, L. Yang, Y. Liu, H. Cui, Antibiotic drug tigecycline inhibits melanoma progression and metastasis in a p21CIP1/Waf1-dependent manner, Oncotarget 7 (2016) 3171–3185, https://doi.org/10.18632/oncotarget.6419.
[54] M. Tolomeo, S. Grimaudo, S. Milano, M. La Rosa, V. Ferlazzo, G. Di Bella, C. Barbera, D. Simoni, P. D'Agostino, E. Cillari, Effects of chemically modified tetracyclines (CMTs) in sensitive, multidrug resistant and apoptosis resistant leukaemia cell lines, Br. J. Pharm. 133 (2001) 306–314, https://doi.org/10.1038/sj.bjp.0704068.
[55] S.H. Kaufmann, S. Desnoyers, Y. Ottaviano, N.E. Davidson, G.G. Poirier, Specific proteolytic cleavage of poly(ADP-ribose) polymerase: an early marker of chemotherapy-induced apoptosis, Cancer Res 53 (1993) 3976–3985.
[56] V. Waetzig, T. Herdegen, A single c-Jun N-terminal kinase isoform (JNK3-p54) is an effector in both neuronal differentiation and cell death, J. Biol. Chem. 278 (2003) 567–572, https://doi.org/10.1074/jbc.M207391200.
[57] A. Ling, I.V. Lundberg, V. Eklof, M.L. Wikberg, A. Oberg, S. Edin, R. Palmqvist, The infiltration, and prognostic importance, of Th1 lymphocytes vary in molecular subgroups of colorectal cancer, J. Pathol. Clin. Res 2 (2016) 21–31, https://doi.org/10.1002/cjp2.31.
[58] H. Raskov, A. Orhan, J.P. Christensen, I. Gogenur, Cytotoxic CD8(+) T cells in cancer and cancer immunotherapy, Br. J. Cancer 124 (2021) 359–367, https://doi.org/10.1038/s41416-020-01048-4.
[59] A. Ibrahim, L.W. Hugerth, L. Hases, A. Saxena, M. Seifert, Q. Thomas, J. A. Gustafsson, L. Engstrand, C. Williams, Colitis-induced colorectal cancer and intestinal epithelial estrogen receptor beta impact gut microbiota diversity, Int J. Cancer 144 (2019) 3086–3098, https://doi.org/10.1002/ijc.32037.
[60] S. Ghanem, C.J. Kim, D. Dutta, M. Salifu, S.H. Lim, Antimicrobial therapy during cancer treatment: Beyond antibacterial effects, J. Intern Med 290 (2021) 40–56, https://doi.org/10.1111/joim.13238.
[61] R. Zhai, X. Xue, L. Zhang, X. Yang, L. Zhao, C. Zhang, Strain-Specific Anti-inflammatory Properties of Two Akkermansia muciniphila Strains on Chronic Colitis in Mice, Front Cell Infect. Microbiol 9 (2019) 239, https://doi.org/10.3389/fcimb.2019.00239.
[62] F. Colombo, O. Illescas, S. Noci, F. Minnai, G. Pintarelli, A. Pettinicchio, A. Vannelli, L. Sorrentino, L. Battaglia, M. Cosimelli, et al., Gut microbiota composition in colorectal cancer patients is genetically regulated, Sci. Rep. 12 (2022) 11424, https://doi.org/10.1038/s41598-022-15230-6.
[63] X. Hou, P. Zhang, H. Du, W. Chu, R. Sun, S. Qin, Y. Tian, Z. Zhang, F. Xu, Akkermansia Muciniphila Potentiates the Antitumor Efficacy of FOLFOX in Colon Cancer, Front Pharm. 12 (2021), 725583, https://doi.org/10.3389/fphar.2021.725583.
[64] G.Y. Koh, A.V. Kane, X. Wu, J.W. Crott, Parabacteroides distasonis attenuates tumorigenesis, modulates inflammatory markers and promotes intestinal barrier integrity in azoxymethane-treated A/J mice, Carcinogenesis 41 (2020) 909–917, https://doi.org/10.1093/carcin/bgaa018.
[65] R. Mirzaei, A. Afaghi, S. Babakhani, M.R. Sohrabi, S.R. Hosseini-Fard, K. Babolhavaeji, S. Khani Ali Akbari, R. Yousefimashouf, S. Karampoor, Role of microbiota-derived short-chain fatty acids in cancer development and prevention, Biomed. Pharm. 139 (2021), 111619, https://doi.org/10.1016/j.biopha.2021.111619.
[66] J. Yang, A. McDowell, E.K. Kim, H. Seo, W.H. Lee, C.M. Moon, S.M. Kym, D.H. Lee, Y.S. Park, Y.K. Jee, et al., Development of a colorectal cancer diagnostic model and dietary risk assessment through gut microbiome analysis, Exp. Mol. Med 51 (2019) 1–15, https://doi.org/10.1038/s12276-019-0313-4.
[67] Y. Wu, N. Jiao, R. Zhu, Y. Zhang, D. Wu, A.J. Wang, S. Fang, L. Tao, Y. Li, S. Cheng, et al., Identification of microbial markers across populations in early detection of colorectal cancer, Nat. Commun. 12 (2021) 3063, https://doi.org/10.1038/s41467-021-23265-y.